Molecular Crystals and Liquid Crystals
Publication details, including instructions for authors and subscription information:
http://www.tandfonline.com/loi/gmcl16

Carrier Transport in van der Waals Solid (II)

Hiroyuki Kitayama [a], Masaaki Yokoyama [a] & Hiroshi Mikawa [a]
[a] Department of Applied Chemistry, Faculty of Engineering, Osaka University, Yamadakami, Suita, Osaka, 565, Japan
Version of record first published: 20 Apr 2011.

To cite this article: Hiroyuki Kitayama , Masaaki Yokoyama & Hiroshi Mikawa (1981): Carrier Transport in van der Waals Solid (II), Molecular Crystals and Liquid Crystals, 76:1-2, 19-34

To link to this article: http://dx.doi.org/10.1080/00268948108074673

Mol. Cryst. Liq. Cryst., 1981, Vol. 76, pp. 19–34
0026-8941/81/7602-0019$06.50/0

Printed in the United States of America

Carrier Transport in van der Waals Solid (II)

II. Carrier Transport Phenomena in 1,3-Diphenyl-5-(*p*-chlorophenyl)-2-pyrozoline

HIROYUKI KITAYAMA, MASAAKI YOKOYAMA and HIROSHI MIKAWA

Department of Applied Chemistry, Faculty of Engineering, Osaka University, Yamadakami, Suita, Osaka, 565 Japan

(*Received December 3, 1980*)

The hole drift mobilities in the different orientations of the single crystal of the title compound were measured by using the time-of-flight method. It was found that the mobility of 2×10^{-2} $cm^2/V.$ sec in the *c*-axis direction is slightly larger than other a^* and *b*-axis directions at room temperature, and a significant change in activation energy was observed at 12°C only in the *c*-axis direction. The anisotropy in drift mobility and the change in activation energy were discussed in terms of the small polaron model. It has been shown that the drift mobilities in the glassy state previously reported can be also explained in terms of the modified small polaron model in the "classical" limit by introducing the ideas of the "effective temperature" and the Poole-Frenkel effect.

INTRODUCTION

Transport phenomena of charge carriers have been of great interest in different aggregations of crystalline, supercooled liquid, or glassy states in van der Waals solids. Excitation energy migration in 1,3-diphenyl-5-(*p*-chlorophenyl)-2-pyrazoline, compound [I], was investigated in such different aggregations.[1] Compound [I] provides one of the suitable materials to be examined, since it gives the aggregations of single crystalline and stable glassy states over a relatively wide temperature range.

In a previous paper,[2] the drift mobilities of holes were measured in the same compound [I] by using the time-of-flight method, and it was found that the hole mobility of approximately 10^{-2} $cm^2/V.$ sec in the single crystalline state was much greater than that measured (10^{-5} $cm^2/V.$ sec) in the glassy state at the room temperature range.

In the present work, the drift mobilities in the different orientations of the

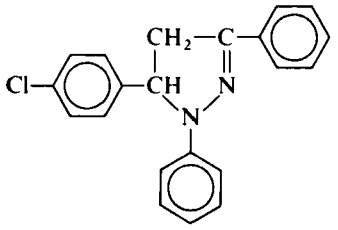

1,3-diphenyl-5-(*p*-chlorophenyl)-2-pyrazoline

[I]

crystal of the compound [I] were measured and significant change in activation energy of the hole drift mobility was observed only in crystallographic *c*-axis. The mobility anisotropy in the single crystal is discussed in detail on the basis of the small polaron theory developed by Holstein[3] and Emin.[4] In addition, it has been shown that the small polaron theory can be applicable to the carrier transport phenomena in the glassy state of compound [I]. The idea of using effective temperature T_{eff}^{-1} ($= 1/T - 1/T_0$) instead of real temperature T in the small polaron theory explained Gill's empirical relation[5] which was observed in various amorphous materials.[5,6]

MEASUREMENTS

Details of the sample preparation, purification and crystal growing procedures of compound [I] have already been reported.[2,7] Although the crystal of [I] has two crystallographic modifications α and β,[8] the melt-grown single crystal used in the present work was the monoclinic α-form. Properly sized single crystal specimens were cut by a diamond cutter into thin disk-like shape (0.05 − 0.1 cm thick) having the specimen surface perpendicular to the crystal axes, a^*, b, c, respectively. The sandwich cell assembly for the drift mobility measurements consists of a transparent conducting Nesa-coated quartz electrode, the well-polished disk-like specimen of [I], and a copper electrode.

Drift mobility was measured by a conventional time-of-flight method. Experimental techniques used in the present measurements were as described in the preceding paper.[2] Only the hole drift mobility was observable in the material.

RESULTS AND DISCUSSION

The temperature dependence of the hole mobility was measured for three kinds of orientations of the crystal, two of them corresponding to the principal crystallographic axes, *b*, *c*, and the other one a^* direction, respectively. Typical data of the hole mobilities as a function of temperature are given in Figure 1, where the logarithms of the mobilities are plotted against the reciprocal of temperature. The mobility was almost independent of the applied electric field ($10^4 - 2.5 \times 10^4$ V/cm) with regard to all crystal orientations. Measurements below −20°C were difficult due to small signals and poorly defined transit times.

Figure 1 indicates that only in the *c*-axis mobility a small but significant change of activation energy appears at ca. 12°C. This behavior was reproducible with different specimens and could not be observed in other orientations. As described in the previous paper,[2] the differential scanning calorimetric measurements of the single crystal specimen showed a change of the baseline at almost the same temperature. Hence, some intramolecular freedom, probably rotational motion of *p*-chlorophenyl side groups, might be released at this temperature, although the details are unknown. The release of intramo-

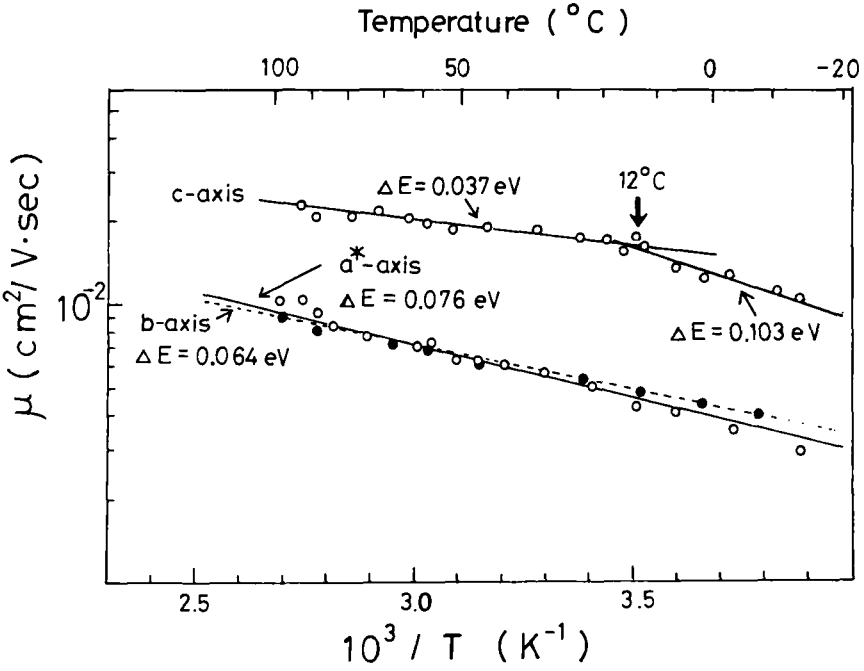

FIGURE 1 Log hole mobility against reciprocal temperature for a^*, *b* and *c* directions.

lecular rotational freedom of a particular group are reported even in crystals from the detailed calorimetric measurements.[9] Figure 2 shows the crystal structure of the compound [I], a projection of the lattice onto the (a^*, b) plane corresponding to a view along the c-axis. It can be seen that p-chlorophenyl groups of the nearest neighboring molecules have good overlap only in this c-axis direction. This would be the reason why the change of the activation energy occurs only in c-axis orientation.

Figure 1 shows also that the drift mobility along the c-axis is slightly greater than that of the b or a^* direction. In order to obtain some information about

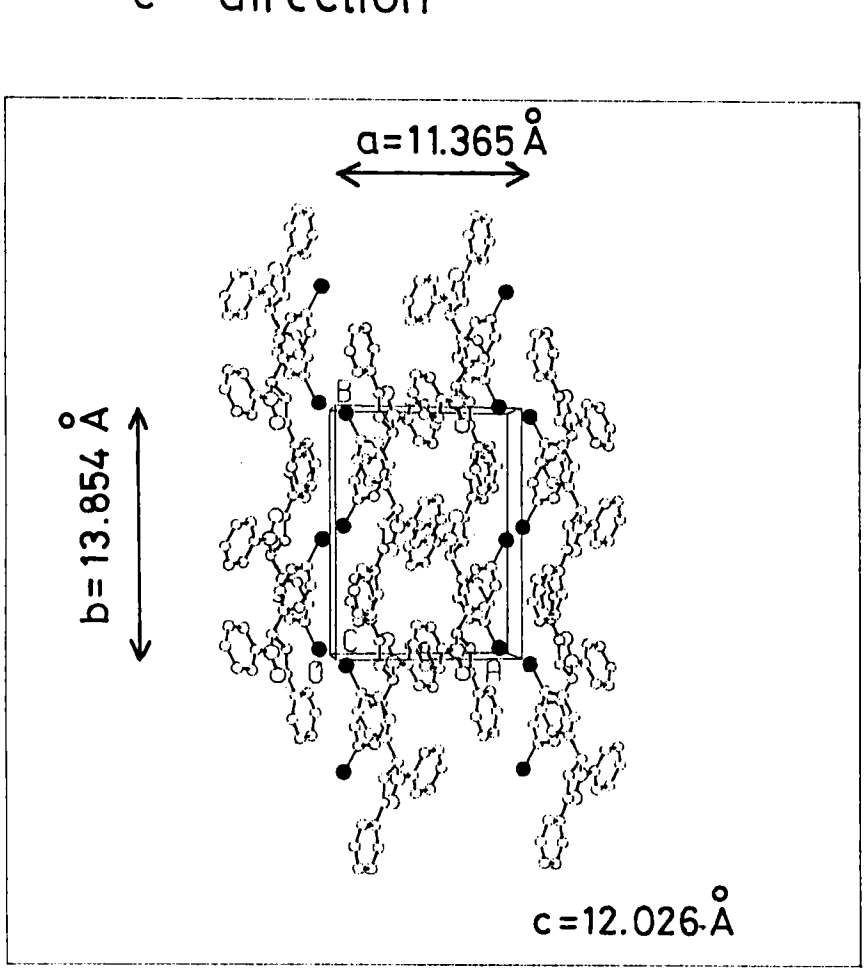

FIGURE 2 Projection of the crystal structure for pyrazoline onto the (a^*, b) plane. The full circles represent the chlorine atoms. Also shown is lattice constant.

TABLE I

The hopping distances and the angles of the orientation between the nearest neighboring molecules of each crystal axis.

direction	hopping distances and angles†
c	(iii) $\xrightarrow[58°]{7.91\ \text{Å}}$ (ii) $\xrightarrow[58°]{7.91\ \text{Å}}$ (iii) + $z\xrightarrow[58°]{7.91\ \text{Å}}$ (ii) + $z\xrightarrow[58°]{7.91\ \text{Å}}$
a^*	(i) $\xrightarrow[58°]{9.37\ \text{Å}}$ (iii) $\xrightarrow[54°]{4.82\ \text{Å}}$ (iv) $\xrightarrow[16°]{9.37\ \text{Å}}$ (ii) $\xrightarrow[0°]{4.82\ \text{Å}}$ (i) + $x\xrightarrow[58°]{9.37\ \text{Å}}$
b	(i) $\xrightarrow[0°]{4.82\ \text{Å}}$ (ii) $\xrightarrow[58°]{7.91\ \text{Å}}$ (iii) $\xrightarrow[54°]{4.82\ \text{Å}}$ (iv) $\xrightarrow[16°]{7.91\ \text{Å}}$ (i) + $y\xrightarrow[0°]{4.82\ \text{Å}}$

† The distances are calculated from the coordinate of nitrogen atom at the 2-position and the angles are given as the angle between the neighboring pyrazoline ring planes. The symbols (i) ~ (iv) are four molecules in a unit cell in the monoclinic α-form pyrazoline,[8] and x, y, z, represent the unit translation to the direction of each crystal axis, a, b, c, respectively.

the paths for carriers to proceed through the molecules, intermolecular distances and orientations between the nearest neighboring molecules are examined from the crystal structural data,[8] and are summarized in Table I. The equidistant alignments were found only in the c-axis direction. In other directions, a^* or b, much shorter intermolecular distance can be found, but poor orientation of π-electron overlap appears in the short path. Thus, the greater drift mobility in the c-axis direction may be understood qualitatively.

Generally, two kinds of well-established models, the band model and the hopping transport model, have been developed as the mechanism of charge carrier transport in semiconductors above and below a value $\sim 1\ \text{cm}^2/\text{V. sec}$ of the drift mobility, respectively.[10] The value of the order of $10^{-2}\ \text{cm}^2/\text{V. sec}$ in the present compound [I] indicates that a description of the carrier transport phenomena in terms of Bloch functions is no longer applicable as reported in most of the organic molecular crystals.[11] In such low drift mobility materials, sometimes a semiempirical expression developed by Böer[12] and Davis *et al.*[13] is used to explain the charge carrier hopping transport based on the phonon-assisted site jumps involving thermally activated tunneling process in the following form:

$$\mu = (e/kT)R^2\nu_p \exp(-2\alpha R) \exp(-W/kt), \tag{1}$$

where ν_p is a phonon frequency, W a measure of the activation energy required for hopping, R, a mean separation of hopping sites and α^{-1} is a characteristic tunneling length, which is a measure of the extent of the wave functions on isolated sites. Since this hopping model represented by Eq. (1) is, however, essentially the same to the small polaron theory developed by Holstein[3] and

Emin,[4] an attempt has been made to apply the original small polaron model to the present material instead of a conventional expression of Eq. (1). The application of the small polaron model was found in various molecular crystals.[14,15]

Drift mobility in crystalline state

The behavior of a small polaron changes from a narrow band type at low temperature to thermally activated hopping due to potential fluctuations induced by lattice vibrations at higher temperatures. The mobility and activation energies increase with increasing temperature.[3] In calculating the transition probablity of a carrier to a neighboring molecular site using time-dependent perturbation theory to a polaron model, Holstein obtained a jumping probability in high-temperature limit;[3]

$$P = (2\pi J^2/h^2\nu)\,[2\pi/2\gamma \text{ cosech } (h\nu/2kT)]^{1/2} \times \exp\{-2\gamma \tanh (h\nu/4kT)\} \quad (2)$$

where J is the intermolecular overlap integral. The dimensionless parameter γ is defined by

$$\gamma = E_b/h\nu \quad (3)$$

where E_b denotes the polaron binding energy and the localized electron (hole) is assumed to interact with a molecular vibrational mode of frequency ν. The corresponding expression for the mobility is obtained by the use of the Einstein relation, $\mu = ea^2P/kT$, where a is the lattice spacing. Eq. (2) can then be written as

$$\mu = (2\pi ea^2J^2/kh)\,f(\nu,\gamma,T) \quad (4)$$

Here, $f(\nu,\gamma,T)$ is defined by

$$f(\nu,\gamma,T) = (1/Th\nu)\{(\pi/2\gamma)[\exp(h\nu/2kT) - \exp(-h\nu/2kT)]\}^{1/2} \times \exp\{-2\gamma[\exp(h\nu/2kT) - 1]/[\exp(h\nu/2kT) + 1]\} \quad (5)$$

Furthermore, this expression of Eq. (4) can be simplified[3] in the "classical" limit of $h\nu/kT \ll 1$;

$$\mu = (2\pi ea^2J^2/kTh)\,(\pi/4kTE_a)^{1/2} \exp(-E_a/kT) \quad (6)$$

where $E_a = E_b/2$ plays a role of activation energy. Thus, in the "classical" limit, we can obtain an expression corresponding to Eq. (1). The condition of "classical" limit is not satisified for transport phenomena in the crystalline state as will be discussed later. The application of Eq. (6) for carrier transport in the glassy state will be discussed later.

The analyses of the charge carrier transport phenomena in the crystalline

state of [I] were made by fitting the experimental data to the theoretical Eq. (4) and determining the parameters ν, γ and J. The values of $f(\nu,\gamma,T)$ given by Eq. (5) were calculated for various ν values and constant values of γ. In Figure 3 are plotted $f(\nu,\gamma,T)$ (as a function of the reciprocal of temperature) for the case of $\gamma = 5$. As can be seen in the figure, there exists a restricted range of ν values to give a straight line showing temperature dependence which corresponds to the experimental activation energy. For a given value of γ, therefore, ν is chosen so as to reproduce the experimental activation energy ΔE obtained for each orientation in Figure 1. Once ν and $f(\nu,\gamma,T)$ are obtained, E_b can be calculated from Eq. (3) and J is estimated from Eq. (4) using the experimental values of drift mobilities μ_{ex}:

$$J = [kh\mu_{ex}/2\pi ea^2 f(\nu,\gamma,T)]^{1/2} \tag{7}$$

Here, the values of the lattice spacing a or a^*, b and c are assumed as 4.82, 4.82 and 7.91 Å, respectively, from Table I.

The results of the above-mentioned curve fitting for each orientation of the crystal are summarized in Table II. The values of J thus obtained are reasonable as compared with the value of 0.05 eV in sulphur[14] and 0.001 − 0.002 eV in anthracene or naphthalene in the c^* direction.[16] The condition for polaron to be stable, that is, $E_b \gg 2J$, is fulfilled for all crystal axes as can be seen in Table II. Table II also shows that the condition, $h\nu/kT \ll 1$, is not satisfied for all crystal orientations investigated, indicating that Eq. (1), which is the "classical" limit of Eq. (6), is not applicable to the charge carrier transport in the crystalline state of the present compound [I]. In order to evaluate the reasonable γ and ν values, the γ values in Table II are plotted in Figure 4 as a function of the reciprocal of the phonon frequency. This figure indicates that γ is proportional to $1/\nu$ for all crystal axes. Since the γ values are reported between 5 and 50,[3,14] then we can estimate the range of the phonon frequencies to be the order of the molecular vibration. It is reasonable to note in Figure 5 that the prominent fundamental peaks of the molecular vibrational spectrum lie between 200 and 300 cm^{-1} corresponding to the values of γ in a range between 5 and 15.

As discussed earlier, in the c-axis direction a small change in activation energy appears at ca. 12°C, and this phenomenon has been tentatively assigned to be due to the release of the frozen rotation of a p-chlorophenyl side group in the crystal at this temperature. From Figure 4 it can be found that the value of γ at $T < 12$°C is larger than that at $T > 12$°C, if the same coupling phonon mode is assumed. From the definition of γ in Eq. (3), the larger γ value gives the larger E_b, and hence at $T < 12$°C the disorder of the p-chlorophenyl groups seems to form the more stable polaron site, and such stable polaron sites would disappear at 12°C due to the release of the frozen rotational freedom.

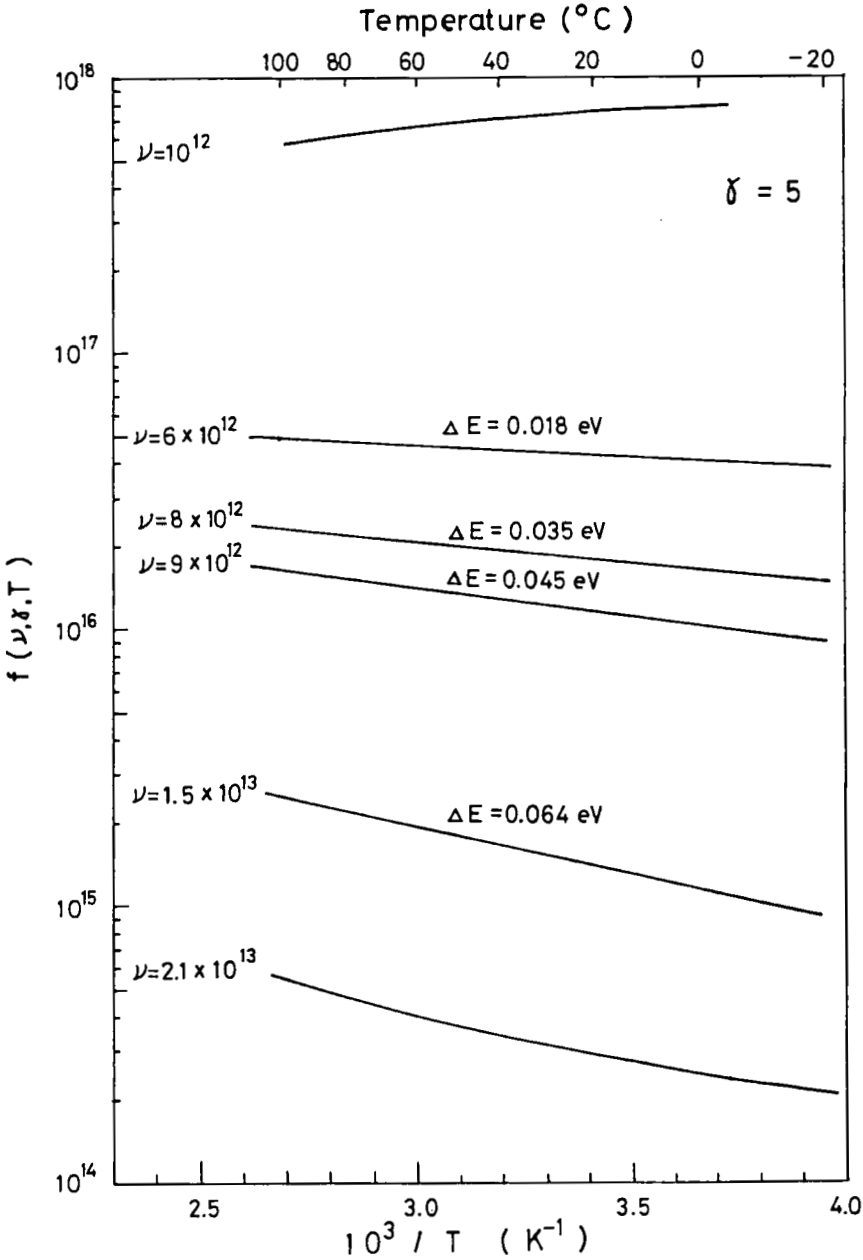

FIGURE 3 Plot of equation (5), $f(\nu, \gamma, T)$ for different values of the frequency parameter ν and constant value of $\gamma = 5$.

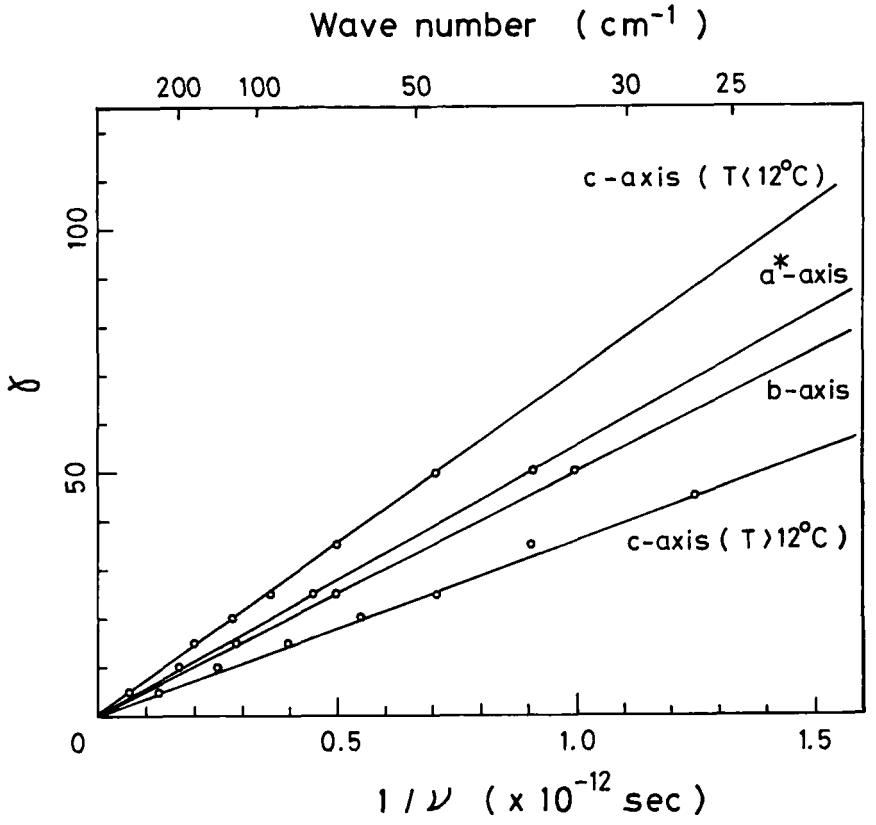

FIGURE 4 Replot of γ of Table II against $1/\nu$.

Mobility in the glassy state

In noncrystalline solids, the localization of charge carriers may occur due to the lack of long range order. The hopping transport through the localized sites requires a predominantly thermal activation process. There are many examples in which the small polaron model was applied to the glassy state, for instance, some chalcogenide glasses containing As and Te[17] and amorphous As_2Se_3,[18] and so on.

Experimentally, the drift mobilities in such noncrystalline glassy states show strong field and temperature dependence, which can be explained by Gill's empirical relation:[5]

$$\mu = \mu_0 \exp\left[-(E_0 - \beta F^{1/2})/kT_{\text{eff}}\right] \tag{8}$$

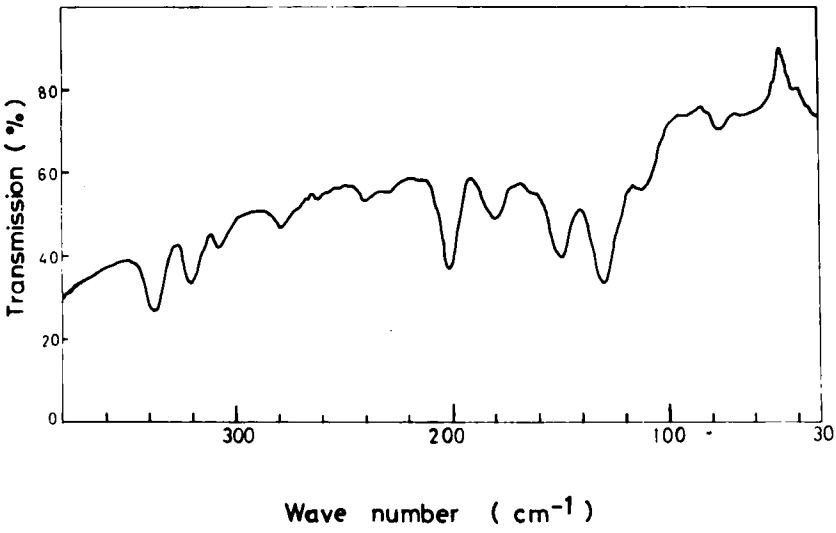

FIGURE 5 Far infrared spectrum for pyrazoline single crystal at 30°C.

TABLE II

Data obtained from the fit of the Holstein theory to the experimental results in the crystalline state.

Axis	γ	ν ($\times 10^{12}$ sec^{-1})	$\bar{\nu}$ (cm^{-1})	E_b (eV)	J (eV)	$E_b/2J$	$h\nu/kT$
c	5	8.0	267	0.167	0.0074	11.3	1.29
($T > 12$°C)	15	2.5	83	0.156	0.0070	11.1	0.40
	25	1.4	47	0.146	0.0063	11.6	0.23
	45	0.8	27	0.150	0.0066	11.4	0.13
c	15	5.0	166	0.313	0.040	3.9	0.97
($T < 12$°C)	25	2.8	93	0.292	0.033	4.4	0.54
	35	2.0	67	0.292	0.033	4.4	0.39
	50	1.4	47	0.292	0.033	4.4	0.27
b	5	15.0	500	0.313	0.0024	65.2	2.42
	15	3.4	113	0.213	0.0012	88.8	0.55
	25	2.0	67	0.208	0.0012	66.7	0.32
	50	1.0	33	0.208	0.0012	86.7	0.16
a^*	10	5.9	197	0.246	0.0016	76.9	0.95
	25	2.2	73	0.229	0.0014	81.1	0.35
	50	1.1	37	0.229	0.0014	80.7	0.18

where F is electric field and

$$1/T_{\text{eff}} = 1/T - 1/T_0 \tag{9}$$

As reported in the previous paper,[2] the experimental values of drift mobilities for the glassy state of our material [I] are well reproduced with this equation with the following values of parameters.

$$\begin{aligned} \mu_0 &= 3.6 \times 10^{-5}\ \text{cm}^2/\text{V. sec} \\ T_0 &= 315\ \text{K (42°C)} \\ E_0 &= 0.63\ \text{eV} \\ \beta_{ex} &= 1.78 \times 10^{-3}\ \text{eV. (V/cm)}^{-1/2} \end{aligned} \tag{10}$$

In order to reproduce the field and temperature dependence of drift mobilities, the Gill empirical equation involves the Poole-Frenkel's effect in activation energy and the idea of the "effective temperature" in place of the real temperature. However, the Gill empirical equation, Eq. (8), is reasonably replaced by Eq. (6) which is derived in the "classical" limit of the small polaron theory except for the above-mentioned points. Thus, it is tempting to interpret Gill's empirical equation with the small polaron model.

First, we attempted to apply the small polaron theory by using the real temperature, but unless an absurd value is chosen as the phonon frequency it is difficult to find the condition, $h\nu/kT \ll 1$, of the "classical" limit in the small polaron theory. Once the "effective temperature T_{eff}" is chosen, however, in place of the real temperature, the condition $h\nu/kT_{\text{eff}} \ll 1$ is satisfied for the glassy state over a wide range of temperature. Although we will discuss the nature of T_{eff} and T_0 later, the introduction of the "effective temperature T_{eff}" allowed the application of Eq. (6) to the charge transport phenomena in the glassy state.

The other important experimental fact in amorphous solids is that the drift mobilities show the Poole-Frenkel type of field-dependence as involved in Gill's relation. To explain such a field-dependence, the following relation is also introduced into Eq. (6):

$$E_a = E_0 - \beta F^{1/2} \tag{11}$$

Here, $E_0 = E_b/2$ (field-independent) in the "classical" limit, and E_a should be regarded as an apparent activation energy.

Under these assumptions, Eq. (6) could be rewritten as

$$\mu_{\text{glass}} = (2\pi e a^2 J^2/kT_{\text{eff}}\hbar)\,[\pi/4kT_{\text{eff}}(E_b/2 - \beta F^{1/2})]^{1/2} \times \exp\,[-(E_b/2 - \beta F^{1/2})/kT_{\text{eff}}] \tag{12}$$

Here, this equation is not applicable to the temperature range near T_0, since

the value of μ approaches zero through a maximum as the increasing temperature approaches T_0.

For the analysis of the data in the glassy state of the present compound [I], $E_b = 1.48$ eV was decided by fitting the experimental data which satisfy Gill's empirical relation[5] to the theoretical Eq. (12) as shown in Figure 6. If the similar molecular vibration of about 6×10^{12} sec^{-1} ($\tilde{\nu} = 200$ cm^{-1}) and a mean jumping distance $a = 8$ Å are reasonably assumed, we obtain $J = 0.000403$ eV and the value of ~ 60 for γ, respectively. These results obtained for the case of the glassy state are summarized in Table III comparing with those for the crystalline state. It should be noted here that the J value in the glassy state is about 20 times smaller than that of the crystalline state, and that the value of

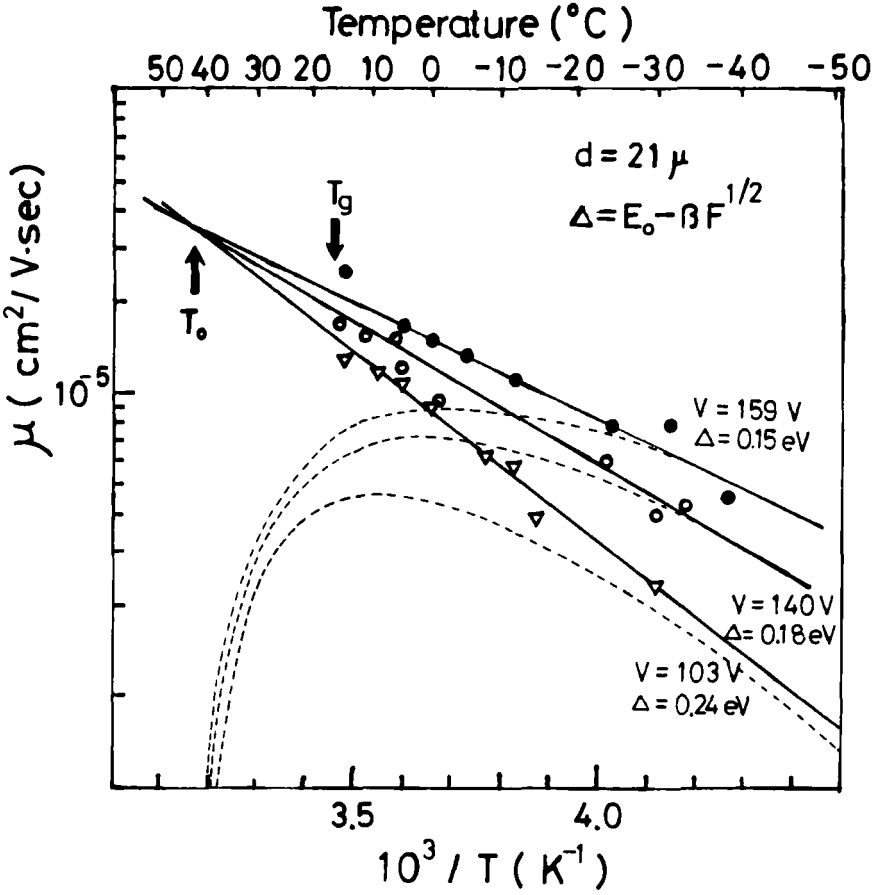

FIGURE 6 Typical experimental data of the hole mobility in the glassy state of compound [I] (——) and the calculated theoretical curve with polaron binding energy $E_b = 1.48$ eV (----).

TABLE III

Data obtained from the small polaron theory to the experimental results in the crystalline and glassy state.

	E_b (eV)	J (eV)	$E_b/2J$	$h\nu/kT$
Crystal	0.15 ~ 0.31	0.001 ~ 0.007	10 ~ 90	0.95 ~ 2.42
Glass	1.48	0.000403	1840	0.07 ~ 0.32

$E_b/2J$ in the glassy state, which is a measure of polaron stability, is much larger than that of the crystalline state.

In addition, by applying Eq. (12) to the glassy state, the physical meaning of μ_0 in Gill's empirical equation can be understood as follows. The pre-exponential factor in Eq. (12) is supposed to correspond to μ_0 in Gill's equation by using T_0 instead of T_{eff} and taking $F = 0$. Under these conditions, μ_0 could be rewritten as

$$(\mu_0)_{\text{theoretical}} = (2\pi ea^2J^2/kT_0h)\,(\pi/2kT_0E_b)^{1/2} \tag{13}$$

From the experimental values of a, j, T_0 and E_b, the values of μ_0 were calculated for the compound [I] and other amorphous materials as shown in Table IV. This table shows that for various amorphous materials the values of $(\mu_0)_{\text{theo}}$ calculated by Eq. (13) are in fair agreement with those of $(\mu_0)_{\text{exp}}$ obtained by experimental data.

Thus, it has been shown that the small polaron theory can explain the charge carrier transport phenomena in the amorphous glassy state by introducing the ideas of the "effective temperature T_{eff}" and the Poole-Frenkel effect. We believe that the modified small polaron theory represented by Eq. (12) will be applicable to a wide range of amorphous glassy materials.

Comparison of the carrier transport in the crystalline and glassy states

The results shown in Table III give us some information about the charge carrier transport phenomena in the crystalline and amorphous glassy states. First, the polaron binding energy E_b and the stability of the polaron in the glassy state are much greater than those in the crystalline state. This fact, of course, indicates that in the glassy state more stable polaron sites can be formed, but it is difficult to consider that at every place in the glass such very stable polarons can be formed because of the lack of even short-range order of molecular alignments. Experimentally, we can detect only the most stable polaron site because such a site will offer the rate determining step in the carrier transport process. In such a stable site, the release from this site should be a field-assisted thermal activation process. Hence, this is the reason why the drift mobilities in the glassy state show field-dependence, and why the Poole-Frenkel effect must be introduced into Eq. (6) of the small polaron model.

TABLE IV

Comparison of $(\mu_0)_{exp}$ in Gill's equation with $(\mu_0)_{theoretical}$ calculated by Eq. (13) for various amorphous materials.

Amorphous materials	E_0 (eV)	E_b (eV)	J (eV)	β eV/(V/cm)$^{1/2}$	a (Å)	T_0 (K)	$(\mu_0)_{exp}$ (cm^2/V·sec)	$(\mu_0)_{theo}$ (cm^2/V·sec)	$\frac{(\mu_0)_{theo}}{(\mu_0)_{exp}}$
Pyrazoline	0.63	1.48	0.000403	0.00178	8	315	3.6×10^{-5}	3.6×10^{-4}	10
PVK(5)	0.65	1.30	0.00264	0.00027	6.5	660	2.0×10^{-2}	3.59×10^{-3}	0.18
TNF(6)	0.63	1.26	0.00519	0.00027	6.8	570	3.9×10^{-2}	1.92×10^{-2}	0.49
1,3-Di-(*N*-carbazolyl)-propane (19)	0.54	1.08	0.00173	0.00038	6.5	450	7.9×10^{-4}	2.98×10^{-3}	3.77
N-isopropylcarbazole doped in polystyrene (19)	0.49	0.98	0.000406	0.00043	7	430	3.8×10^{-5}	2.6×10^{-4}	5.68

Secondly, we introduced the idea of the "effective temperature" into the small polaron theory in the "classical" limit in light of Gill's empirical relation to describe the carrier transport phenomena in the glassy state. The meaning of the "effective temperature" should be discussed, but in the present stage, we have only the following concepts about T_{eff}. In practice, the temperature T_0 in Eq. (9) seems to correspond approximately to the glass transition temperature or melting points in many amorphous materials, for example, in PVK-TNF photoconducting systems,[5] and also in the present case.[2] Thus, T_0 seems to be related to the freezing-in temperature of molecular motion in low molecular weight compounds or of the segmental motion in amorphous polymer materials. As is well-known, the glassy state is thermodynamically a nonequilibrium state, and in such nonequilibrium states the real temperature T might be meaningless. Thus, to describe the thermodynamic phenomena within such nonequilibrium states the "effective temperature T_{eff}," would be required. The accumulation of data in the glassy state will provide more detailed concepts about T_0 and T_{eff}.

Near T_0 of the amorphous material, the glassy state seems to convert into different aggregations, such as the supercooled liquid state, where another carrier transport mechanism plays a predominant role.

In conclusion, the drift mobilities in three orientations of the single crystal of 1,3-diphenyl-5-(*p*-chlorophenyl)-2-pyrazoline were measured and a change in activation energy was found to occur only in the direction of the *c*-axis. The anisotropy in the drift mobility and the change in activation energy were discussed in terms of the small polaron model. It has been shown that the hole drift mobilities in the glassy states can be explained also in terms of the small polaron model in the "classical" limit by introducing the ideas of the "effective temperature T_{eff}" and the Poole-Frenkel effect.

References

1. (a) Y. Sano, K. Kato, M. Yokoyama, Y. Shirota and H. Mikawa, *Mol. Cryst. Liq. Cryst.*, **36**, 137 (1976). (b) Y. Sano, M. Yokoyama, Y. Shirota and H. Mikawa, *Mol. Cryst. Liq. Cryst.*, **53**, 291 (1979).
2. H. Kitayama, M. Yokoyama and H. Mikawa, *Mol. Cryst. Liq. Cryst.*, **69**, 257 (1981).
3. Holstein, *Ann. Phys.*, **8**, 343 (1959).
4. D. Emin, *Adv. Phys.*, **24**, 305 (1975).
5. W. D. Gill, *J. Appl. Phys.*, **43**, 5033 (1972).
6. W. D. Gill, *Energy and Charge Transfer in Organic Semiconductors* (Edited by K. Masuda and M. Silver), p. 137, Plenum Press (1974).
7. K. Kato, M. Yokoyama, Y. Shirota, H. Mikawa, M. Sorai and S. Seki, *Energy and Charge Transfer in Organic Semiconductors* (Edited by M. Masuda and M. Silver), p. 77, Plenum Press (1974).
8. T. Kimura, Y. Kai, N. Yasuoka and N. Kasai, *Acta Cryst.*, B **33**, 1786 (1977).
9. R. E. Pennington, H. L. Finke, W. N. Hubbard, J. F. Messerjy, F. R. Frow, I. A. Hossenlopp and G. Waddington, *J. Am. Chem. Soc.*, **78**, 2055 (1956).
10. H. Fröhlich and G. L. Sewell, *Proc. Phys. Soc.*, **74**, 643 (1959).
11. L. B. Schein, *Phys. Rev.*, **15**, 1024 (1976).

12. K. W. Böer, *J. Non-Cryst. Solid.*, **4**, 583 (1970).
13. E. A. Davis and R. F. Shaw, *J. Non-Cryst. Solid.*, **2**, 406 (1970).
14. D. J. Gibbons and W. E. Spear, *J. Phys. Chem. Solids.*, **27**, 1917 (1966).
15. J. B. Webb and D. F. Williams, *J. Phys. C.*, **11**, 3245, (1978).
16. J. I. Katz, S. A. Rice, S. Choi and J. Jortner, *J. Chem. Phys.*, **39**, 1683 (1963).
17. D. Emin, C. H. Seager and R. K. Quinn, *Phys. Rev. Lett.*, **28**, 813 (1972).
18. G. Pfister and H. Scher, *Phys. Rev. B.*, **15**, 2062, (1977).
19. A. Itaya, K. Okamoto and S. Kusabayashi, private communication.